

# Analysis of the geomagnetic activity of the $D_{st}$ index and self-affine fractals using wavelet transforms

H. L. Wei, S. A. Billings, and M. Balikhin

Department of Automatic Control and Systems Engineering, University of Sheffield, Mappin Street, Sheffield, S1 3JD, UK

Received: 14 January 2004 – Revised: 22 January 2004 – Accepted: 26 April 2004 – Published: 18 June 2004

**Abstract.** The geomagnetic activity of the  $D_{st}$  index is analyzed using wavelet transforms and it is shown that the  $D_{st}$  index possesses properties associated with self-affine fractals. For example, the power spectral density obeys a power-law dependence on frequency, and therefore the  $D_{st}$  index can be viewed as a self-affine fractal dynamic process. In fact, the behaviour of the  $D_{st}$  index, with a Hurst exponent  $H \approx 0.5$  (power-law exponent  $\beta \approx 2$ ) at high frequency, is similar to that of Brownian motion. Therefore, the dynamical invariants of the  $D_{st}$  index may be described by a potential Brownian motion model. Characterization of the geomagnetic activity has been studied by analysing the geomagnetic field using a wavelet covariance technique. The wavelet covariance exponent provides a direct effective measure of the strength of persistence of the  $D_{st}$  index. One of the advantages of wavelet analysis is that many inherent problems encountered in Fourier transform methods, such as windowing and detrending, are not necessary.

## 1 Introduction

The magnetosphere can be considered as a complex input-output system. For such a system, the solar wind plays the role of the input and the geomagnetic indexes can be considered as outputs. Properties of the output data sets can be used to analyse and to understand properties of the dynamical system itself. In the present paper, properties of the  $D_{st}$  index are studied to aid the understanding of properties of the complex magnetospheric dynamical system.

Several approaches have been proposed to analyze the  $D_{st}$  and other geomagnetic indices, see for example the review by Klimas et al. (1996). As time series, these indices have been extensively studied by calculating the auto-correlation, power spectrum, phase-space density and dynamical invariant properties relating to chaotic behaviour, see for example

Baker et al. (1990), Vassiliadis (1990), Shan et al. (1991), Roberts et al. (1991), Takalo et al. (1993, 1995), Chen et al. (1994), Vörös et al. (1994), Takalo and Timonen (1994a, 1994b), Hongre et al. (1997) and Zotov (2000). The  $D_{st}$  index, which is used to measure the disturbance of the geomagnetic field in the magnetic storm, can also be considered as the output of the magnetospheric system with the solar wind as the input. Some simple, effective input-output continuous-time models have been proposed to describe the input-output relationship of the magnetosphere dynamics including Burton's linear model (Burton et al., 1975), the mechanical analogue model by Baker et al. (1990) and Klimas et al. (1997, 1998, 1999), directly driven model by Goertz et al. (1993), the Faraday loop model by Klimas et al., (1996), and the recently proposed model by O'Brien and McPherron (2000). Existing input-output observational data-based modelling approaches which have been applied to these indices include the ARMA model (McPherron, 1999; Vassiliadis et al., 2000), neural networks (Hernandez et al., 1993; Takalo and Timonen, 1997; Wu and Lundsted, 1997), and the NARMAX model (Boaghe et al., 2001).

In this study the fractal invariants of the  $D_{st}$  index are analyzed using wavelet transforms. It is shown that the  $D_{st}$  index possesses properties of self-affine fractals (Vörös et al., 1994), for example, the power spectral density obeys a power-law dependence on frequency, and therefore the  $D_{st}$  index can be viewed as a self-affine fractal dynamic process. Studies of the dynamical invariants of the fractals alone do not reveal the underlying physics. However, the fractal structure of the  $D_{st}$  index does add to the information needed to find the physical mechanism responsible for this phenomenon. The fractal dimension estimated from the power exponent also provides information regarding the choice of an appropriate embedding dimension for the dynamic modelling and forecasting (see, e.g., Hongre et al., 1999) of this index. One of the objectives of this work is to provide an effective alternative approach for the estimation of some dynamical invariants of the  $D_{st}$  index based on the auto-covariance of the wavelet transform.

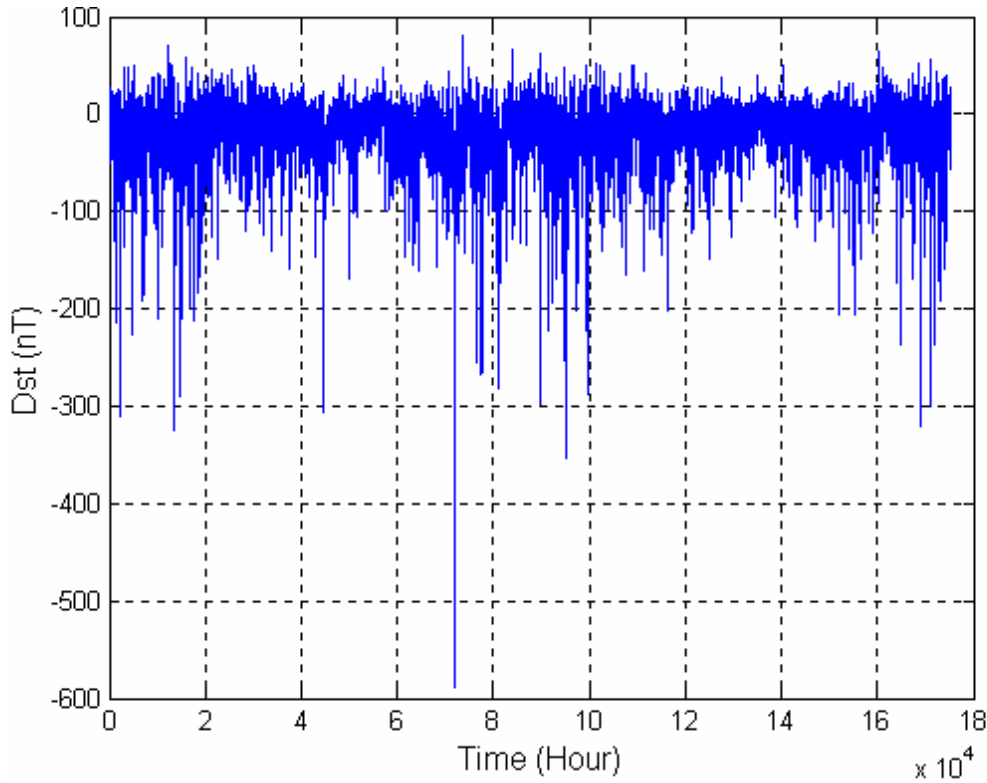


**Fig. 1.** The  $D_{st}$  index for the years from 1981 to 2000 with a sampling period of 1 h.

## 2 The $D_{st}$ index as a self-affine dynamic process

The term fractal, introduced by Mandelbrot (1983), involves three related concepts: geometric, temporal (dynamic) and statistical fractals. Generally, the concept of a fractal is defined in terms of self-similarity. A great number of natural phenomena in physics, geometry, ecology, physiology and topography have been shown to exhibit self-similarity (Fleischmann et al., 1990; Takayasu, 1990; Harrison, 1995).

### 2.1 Self-affine fractals

A self-affine set is statistically invariant under an affine transformation. A 2-dimensional surface described by a function  $f(x, y)$  is a self-affine fractal, if there exists a number  $H$  such that

$$f(x, y) = \lambda^{-H} f(\lambda x, \lambda^H y), \quad (1)$$

where  $\lambda$  is positive numbers,  $H$  is called the Hurst exponent or Hausdorff exponent or self-affine exponent with a value between 0 and 1, that is,  $0 \leq H \leq 1$ . The Eq. (1) indicates that  $f(\lambda x, \lambda^H y)$  is statistically similar to  $f(x, y)$  with a similarity exponent  $H$ . In one-dimension, a self-affine fractal (Mandelbrot, 1983; Turcotte, 1997; Malamud and Turcotte, 1999a, 1999b) is defined as  $f(x) = \lambda^{-H} f(\lambda x)$ . In this case,  $x$  and  $f(x)$  are often interpreted as the time and the corresponding trajectory (position), respectively. It has been proved (Voss, 1988) that the Hurst exponent,  $H$ , and the self-affine fractal dimension, or the box-counting dimension,

$D$ , are related by the equation  $H = 2 - D$ . Therefore  $1 \leq D \leq 2$  corresponds to  $0 \leq H \leq 1$  for a self-affine fractal. If  $H = 1$ , the self-affine fractal becomes self-similar, which is by definition isotropic. A stochastic process or a surface with  $H > 1/2$  is said to be persistent, and that with  $H < 1/2$  is said to be antipersistent.

Following Malamud and Turcotte (1999a, 1999b) and Turcotte (1997), the basic property of a self-affine time series is that the power spectral density of the time series has a power-law dependence on frequency.

## 3 Spectral analysis for the $D_{st}$ index

The physical features of a dynamic system can be easily detected and revealed using frequency domain analysis, which is often implemented by means of Fourier transforms of the covariance functions. One feature of a self-affine time series is that the power spectral density of the time series has a power-law dependence on frequency

$$P(\omega) \propto |\omega|^{-\beta}. \quad (2)$$

Note that for a relationship between the power-law exponent  $\beta$ , the Hurst exponent  $H$ , and the fractal dimension  $D$  is given (Voss, 1988) by  $\beta = 2H + 1 = 5 - 2D$ . For a self-affine process (Malamud and Turcotte, 1999a),  $0 \leq H \leq 1$ ,  $1 \leq D \leq 2$  and  $1 < \beta < 3$ . For a Brownian motion (Malamud and Turcotte, 1999b),  $H = 0.5$ ,  $D = 1.5$  and  $\beta = 2$ .

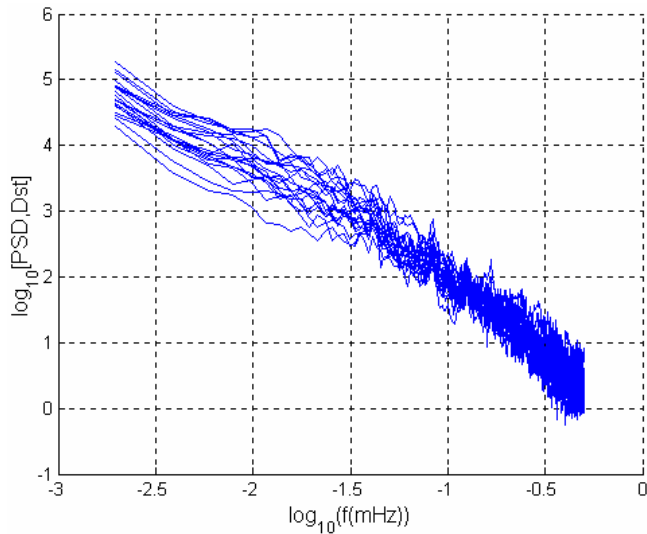


**Fig. 2.** The power spectra of the  $D_{st}$  index for the years from 1981 to 2000 with a sampling period of 1 h for each year index. The slope of the spectral lines is approximately 2.

The main point of this section is to show that the power spectral density of the  $D_{st}$  index obeys a power-law dependence on frequency. As an example, the  $D_{st}$  index for the years from 1981 to 2000 were considered (see Fig. 1) and the power spectra for the  $D_{st}$  index of each year were calculated separately and are shown in Fig. 2, where the sampling period for each yearly index is 1 h and the frequency has been normalised. The average of the 20 power spectral density functions is plotted in Fig. 3 (the solid line). The  $D_{st}$  index over the 20 years can also be considered as a single signal  $s(t)$  consisting of 175 320 points. The power spectrum of this signal was estimated and is also shown in Fig. 3, where again the frequency has been normalised. Figures 2 and 3 clearly show that the power spectra of the  $D_{st}$  index obey a power-law in the sense that  $P(f) \propto |f|^{-\beta}$ , where  $\beta \approx 2 (H \approx 0.5)$ . This suggests that the  $D_{st}$  index can be considered as a self-affine time series and the process of the  $D_{st}$  index is strongly persistent. From the results of Vörös et al. (1994) and Hongre et al. (1999), which demonstrated the chaotic behaviour of the geomagnetic field dynamics, the broadband spectra of the  $D_{st}$  index also indicates that a potential chaotic behaviour may exist in the dynamic process.

A closer inspection of Figs. 2 and 3 also reveals another fact that the power spectrum of the  $D_{st}$  index exhibits some periodicities. In fact, Takalo et al. (1995) showed that there are peaks in the power spectrum at frequencies of about  $1/(6T)$ ,  $1/(8T)$ ,  $1/(12T)$ ,  $1/(24T)$ ,  $1/(648T)$ , where  $T=1$  h. The first 4 peak frequencies are visible in the power spectrum shown in Figs. 2 and 3, but the fifth frequency, which was detected by Takalo et al. (1995) via the structure function (SF), is not visible from the power spectrum. While the peak frequencies  $1/(24T)$  and  $1/(648T)$  can be explained as the results of the diurnal variation and the solar rotation (Takalo et al., 1993), it is difficult to deduce the significant of other peaks from the power spectrum (Takalo et al., 1995).

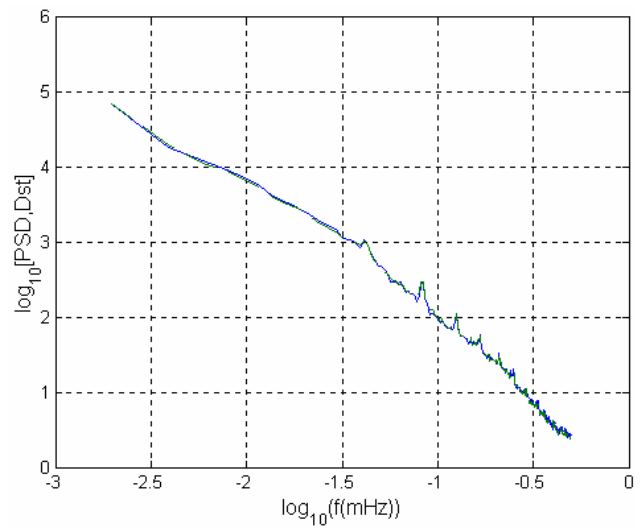


**Fig. 3.** The average of the power spectral density functions of the  $D_{st}$  index for the years from 1981 to 2000 (the solid line) and the overall power spectral density function of the  $D_{st}$  index of 20 years (the dashed line). The average slope of the spectral line is approximately 2.

#### 4 Analysis of the $D_{st}$ index using wavelet transforms and wavelet decompositions

Just as Fourier series can be used to superimpose sines and cosines to represent other functions, wavelets are functions that possess certain properties that can be used to represent complex signals. However, wavelets differ greatly from Fourier series. Unlike the Fourier basis functions, wavelet basis functions have the property of localisation both in time and frequency. Due to this inherent property, wavelet approximation provides the foundation for representing arbitrary signals economically, using just a small number of wavelets. In wavelet analysis, the scale that is used to analyse the data plays a special role.

The wavelet analysis procedure consists of adopting a wavelet prototype function, called the analysing wavelet or mother wavelet or simply wavelet. Temporal analysis is performed with a contracted, high-frequency version of the same function. Because the signal to be analysed can be represented in terms of a wavelet expansion, data operations can be performed using only the corresponding wavelet coefficients.

Wavelets have an excellent approximation capability, that is why wavelet theory has so many applications in many diverse fields, namely signal and image processing, speech analysis, fault detection, fractals, system identification and so on. The wavelet transform also possesses a property of self-similarity. This makes wavelets particularly useful for dealing with nonperiodic and nonstationary multiscaled time series (Holschneider, 1988, 1995), including self-similarity and self-affine signals and fractional Brownian motions (see, e.g., Wornell, 1996; Kumar and Fofoula-Georgiou, 1997; Simonsen, 1998; Malanmud and Turcotte, 1999b).

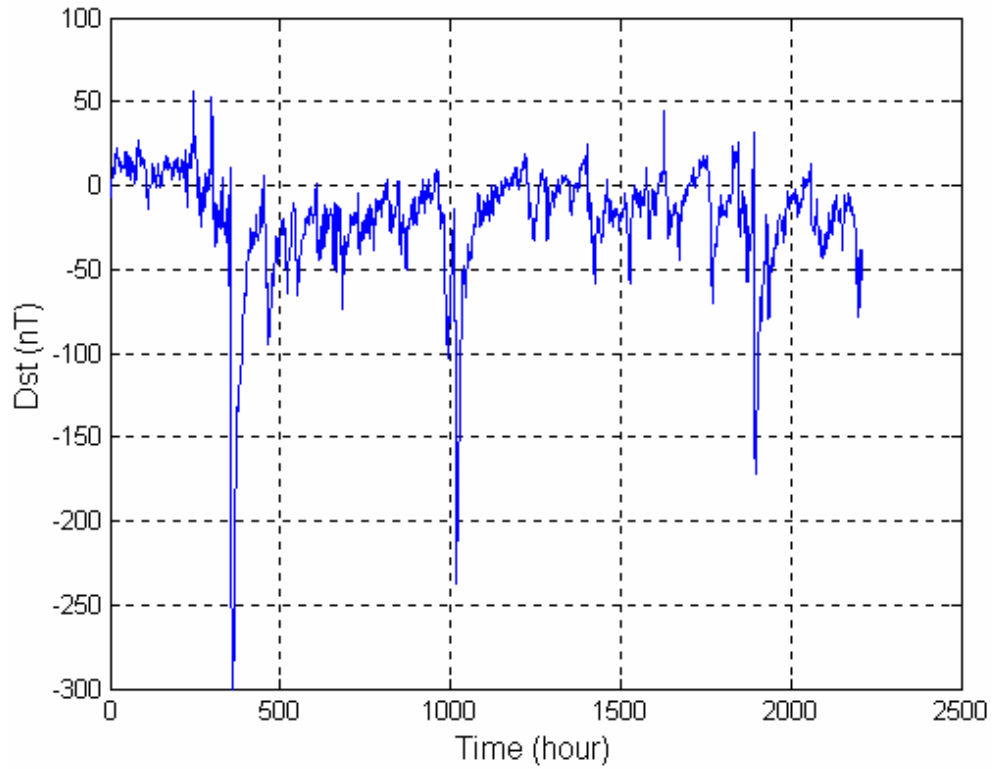


**Fig. 4.** The  $D_{st}$  index for the period from 1 July to 30 September 2000 with a sampling interval of 1 h.

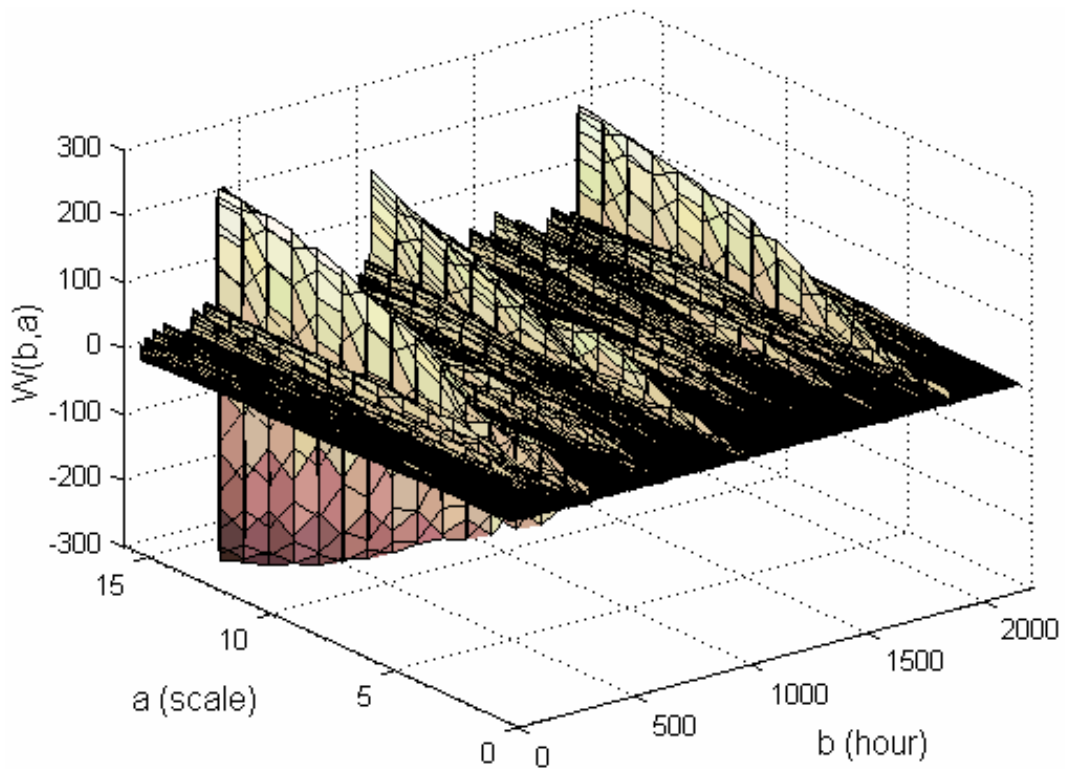


**Fig. 5.** The continuous wavelet transform of the  $D_{st}$  index from 1 July to 30 September 2000, consisting of 2208 data points with a sampling interval of 1 h. The 2nd order Daubechies wavelet (Daub2) was used and the range for the scale parameter  $a$  is  $0.5 \leq a \leq 16$ .

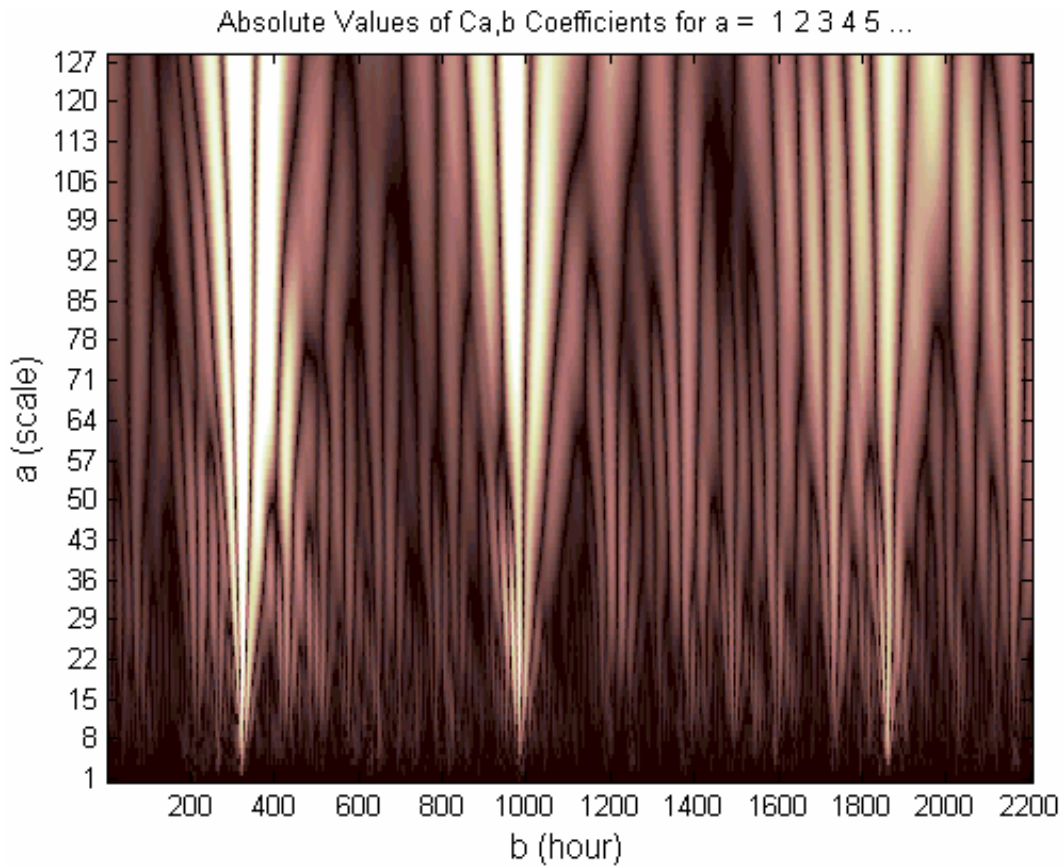


**Fig. 6.** The phase picture of the wavelet transform of the  $D_{st}$  index from 1 July to 30 September 2000, consisting of 2208 data points with a sampling interval of 1 h. The 2nd order Daubechies wavelet (Daub2) was used and the range for the scale parameter  $a$  is  $1 \leq a \leq 128$ .

#### 4.1 Wavelet transforms

Let  $f$  be a function defined in  $L^2(R)$ . The continuous wavelet transform (CWT) with respect to the mother wavelet  $\psi$  is defined as (Chui, 1992; Daubechies, 1992).

$$W_f^\psi(b, a) = \frac{1}{\sqrt{a}} \int_{-\infty}^{+\infty} \overline{f(t)\psi\left(\frac{t-b}{a}\right)} dt, \quad (3)$$

with the dilation (scale) parameter  $a \in R^+$  and the shift (translation) parameter  $b \in R$ . The over-bar above the function  $\psi(\cdot)$  indicates complex conjugate. The Eq. (3) states that the transform  $W_f^\psi(b, a)$  is the correlation of  $f(t)$  with a shifted (by  $b$ ) and scaled (by  $a$ ) version of  $\psi(\cdot)$ . The transform (3) can also be viewed as the output of a filter matched to  $\overline{\psi((t-b)/a)}$ , with the impulse response  $|a|^{-1/2} \overline{\psi((t-b)/a)}$ , at time  $b$  given  $f$  as the input.

It is easy to verify that the continuous wavelet transform (3) possesses the following basic self-similarity property: let  $f \in L^2(R)$  and satisfy  $f(\lambda t) = \lambda^H f(t)$  for a similarity parameter  $H > 0$  and any real number  $\lambda > 0$ , then

$$W_f^\psi(b, a) = \lambda^{-(H+\frac{1}{2})} W_f^\psi(\lambda b, \lambda a). \quad (4)$$

Figure 4 shows the  $D_{st}$  index from 1 July to 30 September 2000, consisting of 2208 data points with a sampling interval

of 1 h. Figure 5 is a 3-D plot showing the wavelet transform (3) of the  $D_{st}$  index from 1 July to 30 September 2000 where the second order Daubechies wavelet (Daub2) was adopted. It can be seen from the Fig. 5 that the wavelet amplitude  $|W_f^\psi(b, a)|$  becomes stronger when the frequency becomes lower (which corresponds to a large scale factor  $a$ ). This is an important feature of a self-affine process (Malamud and Turcotte, 1999b)(The image of the wavelet coefficients for the scale level  $1 \leq a \leq 128$  is shown in Fig. 6.

#### 4.2 Wavelet decompositions

Under some assumptions and considerations, an orthogonal wavelet system can be constructed using a multiresolution analysis (MRA)(Mallat, 1989; Chui, 1992). Assume that the wavelet  $\psi$  and associated scaling function  $\phi$  constitute an orthogonal wavelet system, then any function  $f \in L^2(R)$  can be expressed as a multiresolution wavelet decomposition

$$f(x) = \sum_k a_{j_0,k} \phi_{j_0,k}(x) + \sum_{j \geq j_0} \sum_k d_{j,k} \psi_{j,k}(x), \quad (5)$$

where  $\psi_{j,k}(x) = 2^{j/2} \psi(2^j x - k)$  and  $\phi_{j,k}(x) = 2^{j/2} \phi(2^j x - k)$ ,  $j, k \in Z$ , and the wavelet approximation coefficient  $a_{j_0,k}$  and

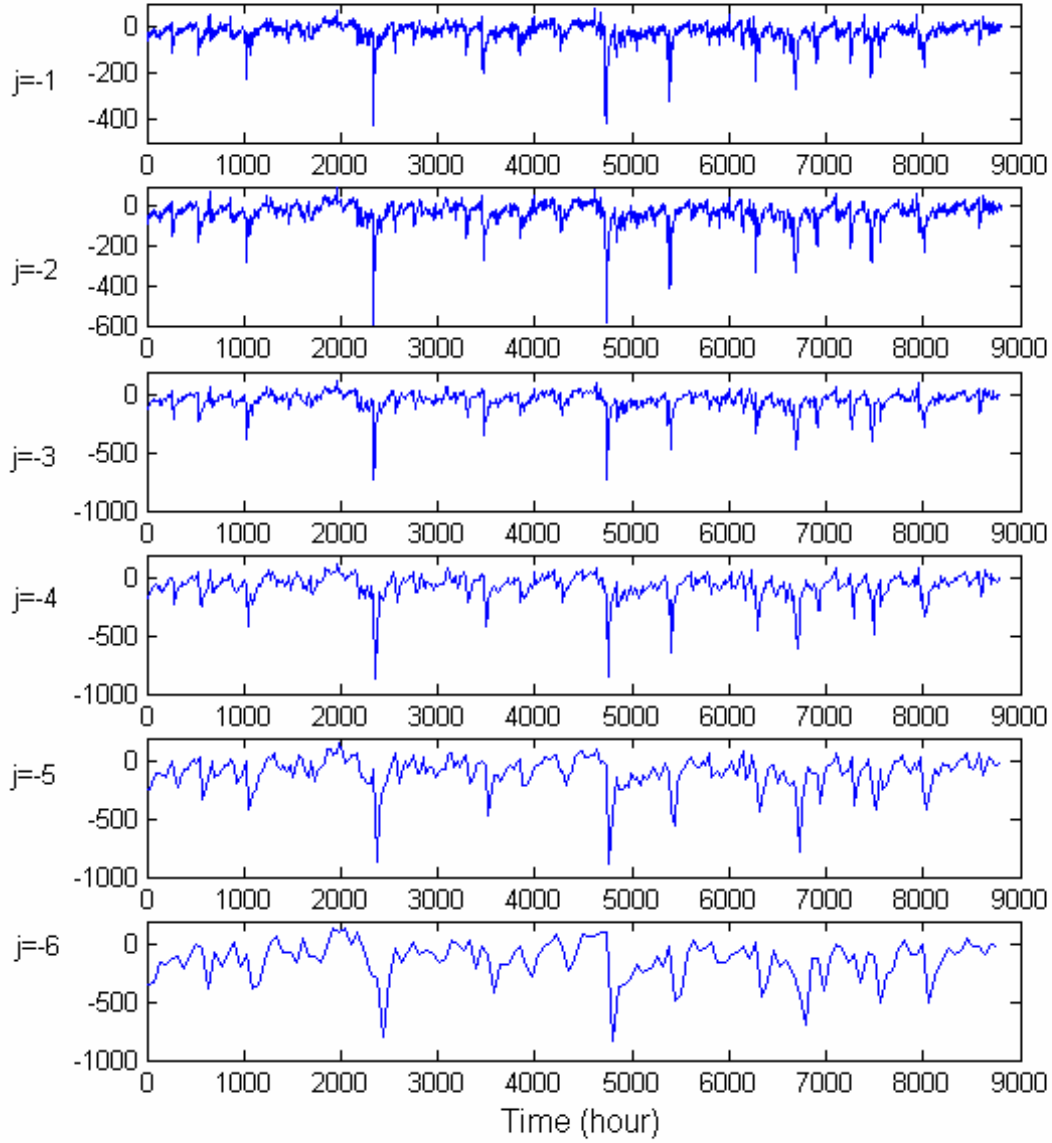


**Fig. 7.** The wavelet approximations at scale  $2^j$  computed with Daub2 for the  $D_{St}$  index of the year 2000, consisting of 8784 data points with a sampling interval of 1 h.

the wavelet detail coefficient  $d_{j,k}$  can be calculated in theory by the inner products:

$$a_{j_0,k} = \langle f, \phi_{j_0,k} \rangle = \int f(x) \overline{\phi_{j_0,k}(x)} dx \quad (6)$$

$$d_{j,k} = \langle f, \psi_{j,k} \rangle = \int f(x) \overline{\psi_{j,k}(x)} dx \quad (7)$$

and  $j_0$  is an arbitrary integer representing the lowest resolution or scaling level.

The  $D_{St}$  index of the year 2000 consisting of 8784 data points with a sampling interval of 1 h was decomposed into the multiresolution wavelet decomposition (5), where the second order Daubechies wavelet (Daub2) was used. The wavelet approximation coefficients  $a_{j,k}$  and the detail coefficients  $d_{j,k}$  are shown in Figs. 7 and 8. Again, it can be

clearly seen from Figs. 7 and 8 that the amplitudes of the wavelet coefficients become stronger when the frequency becomes lower (which corresponds to a large minus  $j$ ). This is an important property of a self-affine process (Malamud and Turcotte, 1999a, 1999b).

#### 4.3 Wavelet transform covariance

Following Flandrin (1989), the covariance of the wavelet transform (3) of a signal  $x(t)$  at a given scale  $a$  can be defined as

$$R_x^\psi(t, s; a) = E \left[ W_x^\psi(t, a) \overline{W_x^\psi(s, a)} \right]. \quad (8)$$

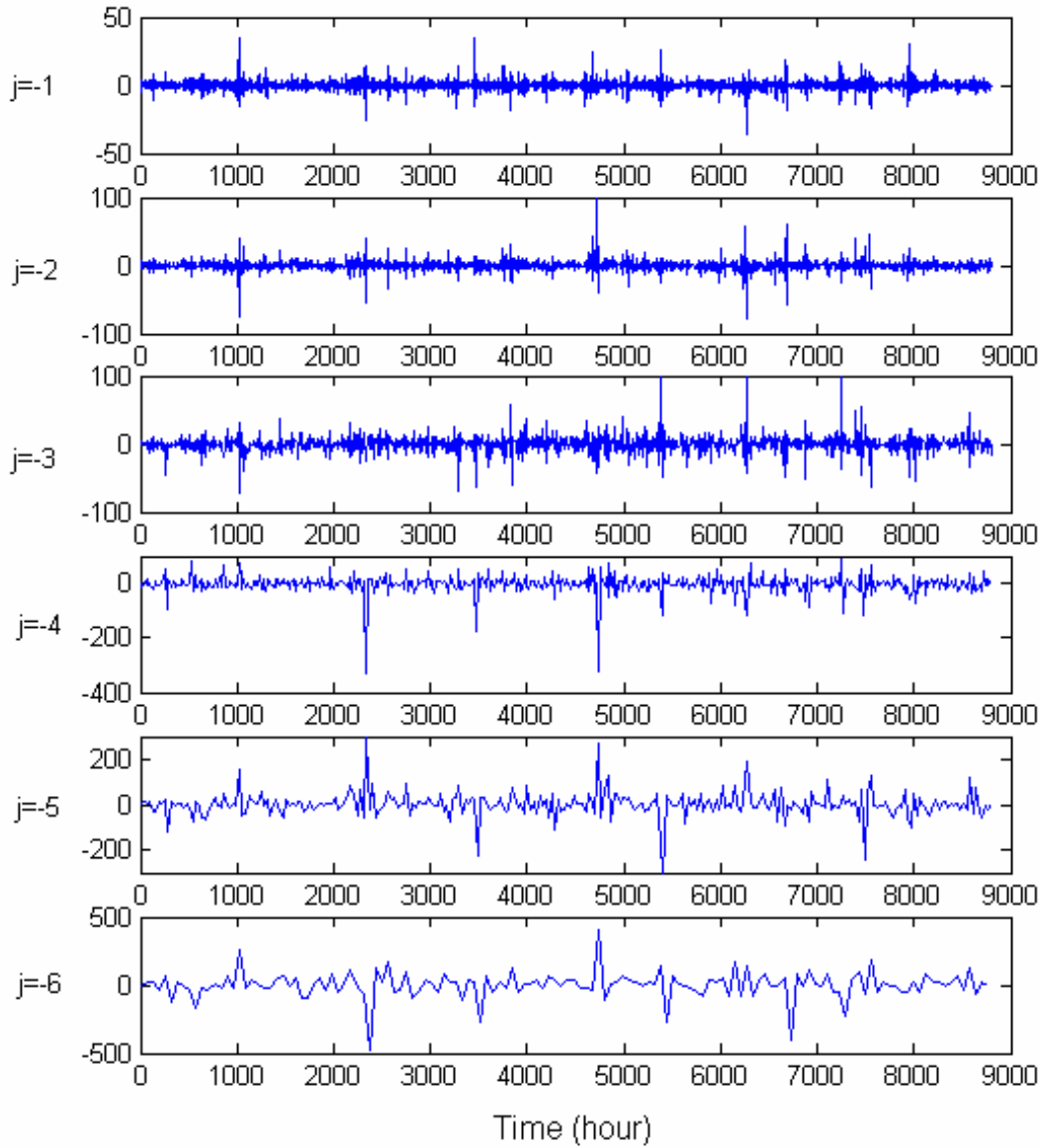


**Fig. 8.** The wavelet details at scale  $2^j$  computed with Daub2 for the  $D_{st}$  index of the year 2000, consisting of 8784 data points with a sampling interval of 1 h.

It can be shown by means of the convolution theory and Parseval’s identity that

$$R_x^\psi(t, s; a) = \frac{a}{2\pi} \int_{-\infty}^{\infty} P_x(\omega) \left| \hat{\psi}(a\omega) \right|^2 e^{-i(t-s)\omega} d\omega \quad (9)$$

where  $P_x(\omega)$  is the power spectrum of the signal  $x(t)$ . If  $x(t)$  is a self-affine signal obeying the power-law (2) with a power exponent  $\beta$ , then the auto-covariance of the wavelet transform also obeys a power-law in the sense that

$$\begin{aligned} R_x^\psi(a) &= E \left[ W_x^\psi(t, a) \overline{W_x^\psi(t, a)} \right] = \frac{a}{2\pi} \int_{-\infty}^{\infty} \frac{\left| \hat{\psi}(a\omega) \right|^2}{|\omega|^\beta} d\omega \\ &= \frac{a^\beta}{2\pi} \int_{-\infty}^{\infty} \frac{\left| \hat{\psi}(\omega) \right|^2}{|\omega|^\beta} d\omega = Ca^\beta, \end{aligned} \quad (10)$$

where  $C = \frac{1}{2\pi} \int_{-\infty}^{\infty} \frac{\left| \hat{\psi}(\omega) \right|^2}{|\omega|^\beta} d\omega$ . Eq. (10) suggests that for a self-affine signal  $x(t)$ , the covariance of the wavelet transform of signal  $x(t)$  also obeys the power-law with respect to the wavelet scale parameter  $a$  and the exponent associated to the wavelet transform covariance is  $\beta$ , which is the same as that of power-law exponent. Therefore, the new introduced formulas (10) can be used to estimate the power-law exponent of the  $D_{st}$  index. The property of the wavelet transform covariance of Brownian motion has been studied in detail by Holschneider (1995) and Malamud and Turcotte (1999a, b).

Figure 9 shows the auto-covariance of the wavelet transform of the  $D_{st}$  index for the years from 1981 to 2000. The slope of the auto-covariance function with respect to the scale factor  $\log_{10} a$  is about 2, which is identical with the power exponent estimated from the power spectral density where the



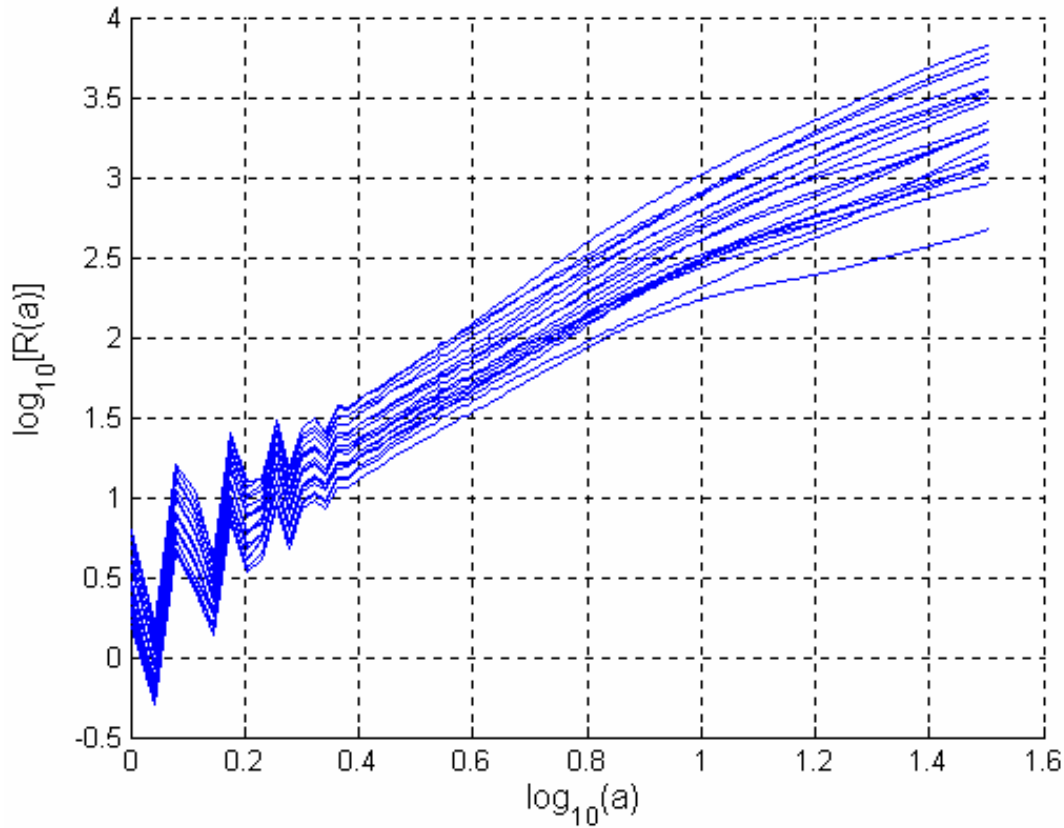


**Fig. 9.** The auto-variance of the wavelet transform of the  $D_{st}$  index for the years from 1981 to 2000, the sampling period for the  $D_{st}$  index of each year is 1 h. The slope of the auto-covariance is approximately  $\beta \approx 2$ . The 4th-order Daubechies wavelet (Daub4) was used and the range for the scale parameter  $a$  is  $1 \leq a \leq 32$ .

value of the slope is approximately  $-2$ . This indicates that the auto-covariance function of the wavelet transform of the  $D_{st}$  index obeys a power-law in the sense that  $R_{D_{st}}^{\psi}(a) \propto |a|^{\beta}$  with  $\beta \approx 2$ . Note that the possible periodicities that appeared in the power spectrum of the  $D_{st}$  index have been filtered out by the wavelet transform and do not occur in the auto-covariance function.

The fractal feature of the  $D_{st}$  index with a power-law exponent  $\beta \approx 2$  (Hurst exponent  $H \approx 0.5$ , the fractal dimension  $D \approx 1.5$ ) suggests that the dynamics of the time series is similar to that of a Brownian motion (see, e.g., Peltier and Levy-Vehel, 1995). This implies that a Brownian motion model might be adopted to describe some aspects of the dynamics of the  $D_{st}$  index. On the other hand, the fractal property possessed by the time series also indicates that the  $D_{st}$  index, as the output of a complex system with the solar wind and other parameters as the inputs, may be sufficiently described using a discrete-time input-output model with a low embedding dimension ( $d = 2D + 1 \approx 4$ ). This provides useful information for modelling the  $D_{st}$  index based only on given observational data sets.

## 5 Conclusions and discussions

The broadband and power-law dependence of the spectrum of the  $D_{st}$  index, identified in this study and in previous work of other authors, clearly show that the  $D_{st}$  index possesses properties associated with self-affine fractals. This suggests that the dynamical invariants of the  $D_{st}$  index might be described by a possible Brownian motion model.

The wavelet transform behaves like a microscope and decomposes a signal into amplitudes depending on dilations (scale) and translation (position). Multi-resolution decomposition enables a signal to be “observed” at higher and higher resolutions at different locations. These features of wavelet transforms along with the property of self-similarity, make wavelets particularly useful for dealing with nonperiodic and nonstationary multiscaled time series, including signals associated with self-affine and self-similar fractals. The power exponent of the  $D_{st}$  index obtained from the wavelet transform covariance is the same as that estimated from the traditional power spectral density. This means that, both the wavelet covariance method and the Fourier transform based power spectral approach give almost the same results for a long data set. However, numerous experiments show that for a short-time signal the wavelet covariance outperforms the Fourier transform based approach. Understanding the



mechanisms of the self-affine fractal of the  $D_{st}$  index is helpful for building either an analogue model or an observational data-driven input-output model for analysis and forecasting of the geomagnetic activity. Wavelet-based input-output nonlinear models can also be estimated and used to predict the  $D_{st}$  index.

As discussed in Sect. 3.3, the proposed wavelet transform covariance provides a direct, effective alternative for analysing some complex invariants of the  $D_{st}$  index. The wavelet transform covariance techniques are likely to be useful for identifying dynamical invariants of other geomagnetic activity indices, as well as the local  $\beta$ -values and a corresponding multifractional Brownian motion model.

*Acknowledgements.* The authors gratefully acknowledge that part of this work was supported by EPSRC. The authors are grateful to Y. Kamide and A. Klimas for providing data. Thanks are given to P. Sailhac and one anonymous reviewer for their constructive and helpful comments to improve the manuscripts.

Edited by: J. Büchner

Reviewed by: K. Sauer and another referee

## References

- Baker, D. N., Klimas, A. J., McPherron, R. L., and Buchner, J.: The evolution from weak to strong geomagnetic activity: an interpretation in terms of deterministic chaos, *Geophys. Res. Lett.*, 17 (1), 41–44, 1990.
- Boaghe, O. M., Balikhin, M. A., Billings, S. A., and Alleyne, H.: Identification of nonlinear processes in the magnetosphere dynamics and forecasting of  $D_{st}$  index, *J. Geophys. Res. Space-Phys.*, 106 (A12), 30 047–30 066, 2001.
- Burton, R. K., McPherron, R. L., and Russell, C. T.: An empirical relationship between interplanetary conditions and  $D_{st}$ , *J. Geophys. Res.*, 80, 4204–4214, 1975.
- Chen, M.W., Lyons, L.R., and Schulz, M. : Simulation of phase-space distributions of storm time proton ring current, *J. Geophys. Res. Space-Phys.*, 99 (A4), 5745–5759, 1994.
- Chui, C. K.: *An Introduction to Wavelets*, Academic Press, Boston, New Jersey, 1992.
- Daubechies, I.: *Ten Lectures on Wavelets*, Society for Industrial and Applied Mathematics, Philadelphia, Pennsylvania, 1992.
- Flandrin, P.: On the spectrum of fractional Brownian motions, *IEEE Trans. Inform. Theory*, 35 (1), 197–199, 1989.
- Fleischmann, M., Tildesley, D. J. and Ball, R. C.: *Fractals in the Nature Sciences-A Discussion*, Princeton University Press, Princeton, 1990.
- Goertz, C. K., Shan, L. H., and Smith, R. A.: Prediction of geomagnetic activity, *J. Geophys. Res. Space-Phys.*, 98 (A5), 7673–7684, 1993.
- Goldberger, A. L.: Fractal mechanisms in the electrophysiology of heart. *IEEE Engineering in Medicine and Biology Magazine*, 11 (2), 47–52, 1992.
- Harrison, A.: *Fractals in Chemistry*, Oxford University Press, Oxford, 1995.
- Hernandez, J. V., Tajima, T., and Horton, W.: Neural net forecasting for geomagnetic activity, *Geophys. Res. Lett.*, 20 (23), 2707–2710, 1993.
- Holschneider, M.: On the wavelet transforms of fractal objects, *Journal of Statistical Physics*, 50 (5-6), 953–993, 1988.
- Holschneider, M.: *Wavelets: An Analysis Tool*, Clarendon Press, Oxford, 1995.
- Hongre, L., Sailhac, P., Alexandrescu, M., and Dubois, J.: Nonlinear and multifractal approaches of the geomagnetic field, *Physics of the earth and planetary interiors*, 110 (3-4), 157–190, 1997.
- Klimas, A. J., Vassiliadis, D., Baker, D. N.: Data-derived analogues of the magnetospheric dynamics, *J. Geophys. Res. Space-Phys.*, 102 (A12), 26 993–27 009, 1997.
- Klimas, A. J., Vassiliadis, D., Baker, D. N.:  $D_{st}$  index prediction using data-derived analogues of the magnetospheric dynamics, *J. Geophys. Res. Space-Phys.*, 103 (A9), 20 435–20 447, 1998.
- Klimas, A. J., Vassiliadis, D., Baker, D. N., and Roberts, D. A.: The organized nonlinear dynamics of the magnetosphere, *J. Geophys. Res. Space-Phys.*, 101 (A6), 13 089–13 113, 1996.
- Klimas, A. J., Vassiliadis, D., Baker, D. N., and Valdivia J. A.: Data-derived analogues of the solar wind magnetosphere interaction. *Physics and Chemistry of the Earth, Part C*, 24 (1-3), 37–44, 1999.
- Kumar, P. and Foufoula-Georgiou, E.: Wavelet analysis for geophysical applications, *Reviews of Geophysics*, 35 (4), 285–412, 1997.
- Malamud, B. D. and Turcotte, D. L.: Self-affine time series, I: Generation and analyses, *Advances in Geophysics*, 40, 1–90, 1999a.
- Malamud, B. D. and Turcotte, D. L.: Self-affine time series: measures of weak and strong persistence, *Journal of Statistical Planning and Inference*, 80 (1-2), 173–196, 1999b.
- Mallat, S. G.: A theory for multiresolution signal decomposition: the wavelet representation, *IEEE Trans. on Pattern analysis and machine intelligence*, 11 (7), 674–693, 1989.
- Mandelbrot, B. B.: *The Fractal Geometry of Nature*, W. H. Freeman and Company, San Francisco, New York, 1983.
- McPherron, R. L.: Predicting the  $A_p$  index from past behaviour and solar wind velocity, *Physics and Chemistry of the Earth, Part C*, 24 (1-3), 45–56, 1999.
- O'Brien, T. P. and McPherron, R. L.: An empirical phase space analysis of ring current dynamics: solar wind control of injection and decay, *J. Geophys. Res. Space-Phys.*, 105 (A4), 7707–7719, 2000.
- Peltier, R. F. and Levy-Vehel, J.: Multifractal Brownian motion: Definition and preliminary results, *INRIA Report No. 2645*, (<http://www.inria.fr/rrrt/tr-2645.html>), 1995.
- Roberts, D. A., Baker, D. N, and Klimas, A. J.: Indications of low-dimensionality in magnetosphere dynamics, *Geophys. Res. Lett.*, 18 (2), 151–154, 1991.
- Shan, L. H., Hansen, P., Goertz, C. K., and Smith, R. A.: Chaotic appearance of the AE index, *Geophys. Res. Lett.*, 18 (2), 147–150, 1991.
- Sahimi, M.: Fractal-wavelet neural-network approach to characterization and upscaling of fractal reservoirs, *Computers & Geosciences*, 26 (8), 877–905, 2000.
- Simonsen, I., Hansen, A., and Nes, O. M.: Determination of the Hurst exponent by use of wavelet transforms, *Physical Review E*, 58 (3), 2779–2787, 1998.
- Takalo, J. and Timonen, J.: Characteristic time-scale of auroral electronjet data, *Geophys. Res. Lett.*, 21 (7), 617–620, 1994a.
- Takalo, J. and Timonen, J.: Properties of AE data and bicolored noise, *Journal of Geographical Research*, 99, 13 239–13 249, 1994b.
- Takalo, J. and Timonen, J.: Neural network prediction of AE data, *Geophys. Res. Lett.*, 24 (19), 2403–2406, 1997.

- Takalo, J., Lohikosiki, R., and Timonen, J.: Structure function as a tool in AE and  $D_{st}$  time series analysis, *Geophys. Res. Lett.*, 22 (5), 635–638, 1995.
- Takalo, J., Timonen, J., and Koskinen, H.: Correlation dimension and affinity of AE data and bicolored noise, *Geophys. Res. Lett.*, 20 (15), 1527–1530, 1993.
- Takayasu, H.: *Fractals in the Physical Sciences*, Manchester University Press, Manchester, 1990.
- Turcotte, D. L.: *Fractals and Chaos in Geology and Geophysics* (2nd Ed.), Cambridge University Press, Cambridge, 1997.
- Vassiliadis, D., Sharma, A. S., Eastman, T. E., and Papadopoulos, K.: Low-dimensional chaos in magnetospheric activity from AE time series, *Geophys. Res. Lett.*, 17 (11), 1841–1844, 1990.
- Vassiliadis, D., Klimas, A. J., Valdivia, J. A., and Baker, D. N.: The nonlinear dynamics of space weather, *Physics and Chemistry of the Earth, Part C*, 26 (1), 197–207, 2000.
- Voss, R. F.: Fractals in nature: from characterization to simulation, in: *The Science of Fractals Images*, edited by Peitgen, H. O. and Saupe, D., Springer, New York, 1988.
- Vörös, Z., Verö, J., and Kristek, J.: Nonlinear time series analysis of geomagnetic pulsations, *Nonl. Proc. Geophys.*, 1, 145–155, 1994.
- Wornell, G. W.: *Signal Processing with Fractals : a Wavelet-based Approach*, Prentice Hall PTR, New Jersey, 1996.
- Wu, J. G. and Lundsted, H.: Neural network modelling of solar wind magnetosphere interaction, *J. Geophys. Res. Space-Phys.*, 102 (A7), 14 457–14 466, 1997.
- Zotov, O. D.: Self-affine fractal dynamics of solar and earth magnetospheric activities, *Geomagnetism and Aeronomy*, 40 (4), 439–443, 2000.